ARTICLE

doi:10.1038/nature10674

A disinhibitory microcircuit for associative fear learning in the auditory cortex

Johannes J. Letzkus[1]*, Steffen B. E. Wolff[1,2]*, Elisabeth M. M. Meyer[1,2], Philip Tovote[1], Julien Courtin[3], Cyril Herry[3] & Andreas Lüthi[1]

Learning causes a change in how information is processed by neuronal circuits. Whereas synaptic plasticity, an important cellular mechanism, has been studied in great detail, we know much less about how learning is implemented at the level of neuronal circuits and, in particular, how interactions between distinct types of neurons within local networks contribute to the process of learning. Here we show that acquisition of associative fear memories depends on the recruitment of a disinhibitory microcircuit in the mouse auditory cortex. Fear-conditioning-associated disinhibition in auditory cortex is driven by foot-shock-mediated cholinergic activation of layer 1 interneurons, in turn generating inhibition of layer 2/3 parvalbumin-positive interneurons. Importantly, pharmacological or optogenetic block of pyramidal neuron disinhibition abolishes fear learning. Together, these data demonstrate that stimulus convergence in the auditory cortex is necessary for associative fear learning to complex tones, define the circuit elements mediating this convergence and suggest that layer-1-mediated disinhibition is an important mechanism underlying learning and information processing in neocortical circuits.

The transformation of sensory input to an appropriate behavioural output is accomplished by neuronal circuits that process information through dynamic interactions between distinct types of neurons. Learning as an adaptive change of an animal's behaviour modifies these network computations. Important cellular mechanisms underlying learning are thought to be activity-dependent synaptic plasticity[1] and subsequent structural modifications[2]. In contrast to our detailed understanding of these cellular mechanisms, the factors and circuit elements controlling neuronal activity and concomitant induction of plasticity during learning in the intact animal remain poorly understood.

Neocortical interneurons exert powerful control over circuit activity by supplying inhibition to surrounding pyramidal neurons and to other interneurons[3]. The balance of excitation and inhibition is critical to circuit function, and is maintained under most conditions including sensory stimulation, when thalamocortical input typically recruits feed-forward inhibition a few milliseconds after direct excitation[4,5]. This form of inhibition is mainly supplied by basket cells, the most abundant type of interneuron in the rodent neocortex[3]. Fast-spiking basket cells establish strong synapses with high release probability on the perisomatic region of pyramidal neurons where they control firing, and express the calcium-binding protein parvalbumin (PV)[3,6,7].

On top of the glutamatergic recruitment of inhibition by sensory input, several types of interneurons are also major targets of neuromodulation[8–11], suggesting that these systems can profoundly affect circuit computations by shifting the excitation–inhibition balance[12]. This has mainly been addressed *in vitro*, revealing a staggering complexity of effects which strongly depend on interneuron type[8–11]. Given that neuromodulation has a key role in learning[13,14], it is likely that interneurons are engaged in these processes. However, the contribution of different interneuron types to learning in the intact animal remains elusive.

Auditory fear conditioning is a form of associative learning acquired by temporal coincidence of a neutral conditioned stimulus (CS, a tone) with a mild foot shock. Fear conditioning causes prominent, long-lasting plasticity of CS responses in auditory cortex[13–15], which depends on the activity of cholinergic afferents from the basal forebrain[13,14,16]. Pairing of tones with basal forebrain stimulation can elicit similar plasticity in auditory cortex[13,14], and a recent study suggests an involvement of pyramidal neuron disinhibition in this process[17]. Here, we investigate the contribution of identified types of auditory cortex interneurons to acquisition of auditory fear memory. Our results indicate that foot shocks, via recruitment of cholinergic basal forebrain afferents, activate a disinhibitory neocortical microcircuit that is required for fear learning.

Nicotinic activation of L1 interneurons by foot shocks

Fear memory acquisition critically depends on the amygdala[18]. In contrast, the role of auditory cortex is contentious, with evidence both for[19,20] and against an essential function in auditory fear conditioning[19,21]. Based on the hypothesis that stimulus complexity determines the engagement of neocortex[18], we performed differential fear conditioning using trains of upward and downward frequency-modulated sweeps as the CS (Fig. 1a, modulation between 5 and 15 kHz). To test directly the role of auditory cortex in this paradigm, we inhibited neuronal activity during fear conditioning by local injection of the $GABA_A$ (γ-aminobutyric acid)-receptor agonist muscimol into the auditory cortex (Fig. 1a and Supplementary Fig. 1). When tested 24 h later in a drug-free state, this manipulation resulted in strongly reduced fear levels (Fig. 1b), indicating that activity in auditory cortex is required for fear learning in this paradigm.

We next focused on the circuit mechanisms underlying acquisition of fear memory in the auditory cortex (defined here as areas A1 and AuV). The role of the auditory cortex could be that of an essential relay for tone information to downstream structures like the amygdala. Alternatively, foot shocks alone might also elicit activity in the auditory cortex, and convergence of tone and foot-shock information during fear conditioning could then contribute to fear learning. To distinguish these alternatives, we used two-photon calcium imaging of neurons in

[1]Friedrich Miescher Institute for Biomedical Research, Maulbeerstrasse 66, CH-4058 Basel, Switzerland. [2]University of Basel, CH-4003 Basel, Switzerland. [3]INSERM U862, Neurocentre Magendie, 146 Rue Léo-Saignat, 33077 Bordeaux, France.
*These authors contributed equally to this work.

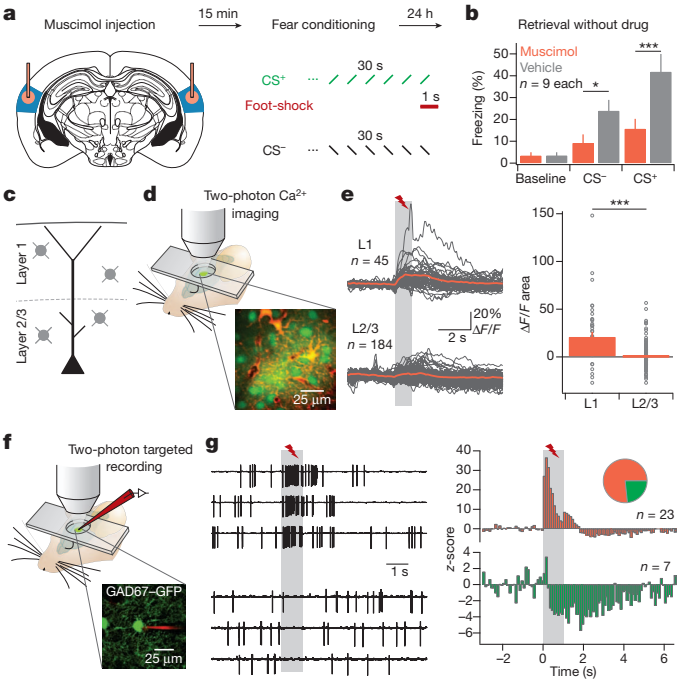

Figure 1 | Foot-shock responses in auditory cortex L1 interneurons. **a**, Left, injection of the $GABA_A$-receptor agonist muscimol (red) into the auditory cortex (blue). Right, differential fear-conditioning protocol using frequency-modulated sweeps. **b**, Drug-free freezing 1 day after conditioning in a new context. Compared to vehicle-injected mice (grey), muscimol reduced freezing to both CS^- and CS^+ (red). **c**, Cytoarchitecture of upper layers of auditory cortex (interneurons grey, pyramidal neuron black). **d**, Two-photon calcium imaging in head-fixed, anaesthetized mice using OGB-1 AM (green) and sulforhodamine 101 (red, counterstains glial cells). **e**, Left, responses in L1 and L2/3 to foot shocks in single neurons (grey) and the population average (red). Right, L1 interneurons display much stronger activation than L2/3 neurons. **f**, Two-photon targeted loose-seal cell-attached recording of L1 interneuron (green). **g**, Example traces (left) and *z*-scored population peri-stimulus time histograms (right) of two types of foot-shock responses in L1 interneurons. Inset, incidence of response type. Values are mean ± s.e.m. $*P < 0.05$, $***P < 0.001$. Statistical analysis in Supplementary Information.

the superficial layers of the auditory cortex in mice anaesthetized with chlorprothixene and urethane (Fig. 1c, d). Trains of frequency-modulated sweeps used as the CS strongly activated neurons in layer 2/3 (L2/3, Supplementary Fig. 2), whereas mild foot shocks applied to the hindpaws evoked little response (Fig. 1e and Supplementary Fig. 2). In marked contrast, the population of neurons located in L1 displayed strong activation by foot shocks (Fig. 1e). Layer 1 is unique in the neocortex because it contains only very few neuronal somata, almost all of which are GABAergic interneurons[22–25]. To investigate their activation in more detail, we used two-photon targeted loose-seal cell-attached recordings[26] (Fig. 1f). These experiments showed that L1 interneurons are tonically active (baseline frequency 3.2 ± 0.5 Hz, $n = 30$), and confirmed that the majority of L1 interneurons are strongly activated by foot shocks, while a minority (23%) displayed inhibition during and after foot shocks (Fig. 1g and Supplementary Fig. 3). The excitatory response was also present when foot shocks were paired with tones, whereas L1 interneurons did not show pronounced responses to tones alone (Supplementary Fig. 4). Interestingly, we observed a very similar activation of L1 interneurons by foot shocks in the primary visual cortex (Supplementary Fig. 5), indicating that the relevance of this pathway may extend beyond auditory memory acquisition.

Layer 1 is a prominent feedback pathway in the neocortex, containing both glutamatergic projections from higher cortical areas[27,28] (and from non-specific thalamic nuclei[29]) and cholinergic afferents from the basal forebrain, the major source of acetylcholine in the rodent neocortex[14,30–32]. We next sought to identify the afferent pathways mediating activation of L1 interneurons during foot shocks. Local bath-application of the glutamate receptor antagonist NBQX (1 mM) strongly reduced baseline firing frequency (Supplementary Fig. 6), but left the foot-shock response in L1 interneurons intact (Fig. 2a, b and Supplementary Fig. 6, see below). In contrast, combined application of the nicotinic acetylcholine receptor (nAChR) antagonists mecamylamine and methyllycaconitine (1 and 0.1 mM, respectively) abolished the L1 interneuron response almost completely (Fig. 2c and Supplementary Fig. 6), and drastically reduced baseline firing (Supplementary Fig. 6). In agreement with the interpretation that cholinergic basal forebrain afferents generate foot-shock responses in L1 interneurons, electrical microstimulation of the basal forebrain caused strong excitation of L1 interneurons in the absence of foot shocks (Fig. 2d and Supplementary Fig. 6). Activation of the basal forebrain by foot shocks is expected to have a longer latency than thalamocortical signalling[14]. Latency analysis showed that L1 interneuron activation was biphasic, with an early, glutamatergic peak (onset 10 to 20 ms after shock onset) which may originate from non-lemniscal thalamus[29], and a later, nicotinic peak (onset 40 to 50 ms after shock onset) that outlasted the foot shock and contained the majority of spikes (Fig. 2 insets). As previously reported[24], recordings from brain

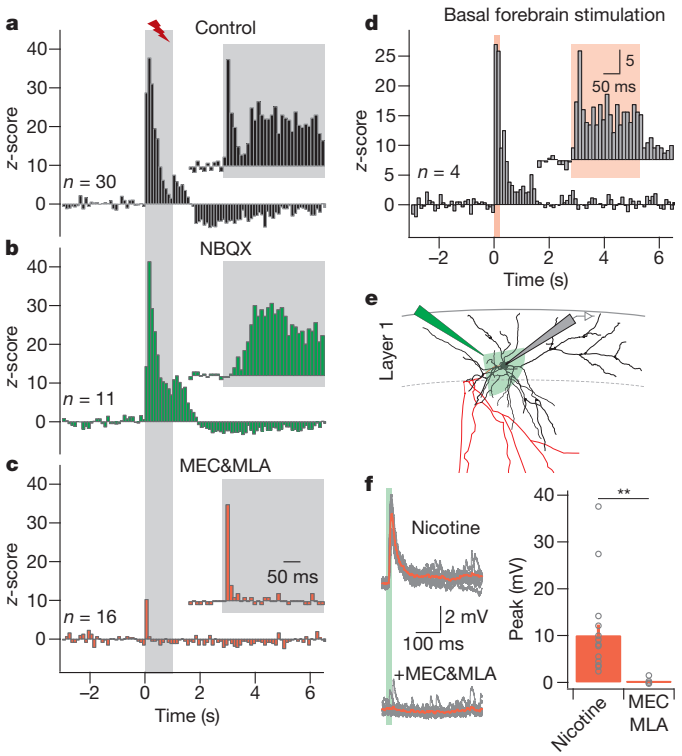

Figure 2 | Nicotinic activation of L1 interneurons by foot shocks. **a**, Population response of L1 interneurons to foot shocks. Insets in **a**–**d** are at high temporal resolution (10-ms bins). The control response was biphasic (onset 10–20 ms after foot-shock onset). **b**, Local application of the glutamate receptor antagonist NBQX left the response intact, but selectively eliminated the early peak, indicating its glutamatergic nature (inset, onset latency 40–50 ms). **c**, Local block of nAChRs by mecamylamine and methyllycaconitine (MEC&MLA) strongly reduced foot-shock responses, selectively eliminating the later, broader peak (inset). **d**, Electrical microstimulation of the basal forebrain activated L1 interneurons after 10 to 20 ms (inset, $n = 4$). **e**, Whole-cell recording of a L1 interneuron (black, soma and dendrites; red, axon) in auditory cortex slices during puff application of nicotine (100 µM, 20 ms). **f**, Left, example nicotine responses in control and after bath-application of mecamylamine (100 µM) and methyllycaconitine (0.1 µM; grey, single trials; red, average). Right, all L1 interneurons displayed nicotine responses ($n = 17$), which were blocked by the nAChR antagonists ($n = 8$). Values are mean ± s.e.m. $**P < 0.01$. Statistical analysis in Supplementary Information.

slices showed that all L1 interneurons showed responses to nicotine puffs (Fig. 2e, f) that were blocked by the same antagonists that abolished foot-shock responses *in vivo* (Fig. 2f), and could fire L1 interneurons (Supplementary Fig. 7). In summary, these results indicate that activity of cholinergic basal forebrain neurons is both necessary and sufficient to fire L1 interneurons during foot shocks, and that acetylcholine activates nAChRs on L1 interneurons. This implies that acetylcholine is released rapidly (<50 ms) after an aversive stimulus. Activation of L1 interneurons in turn is likely to have a central role in fear-conditioning-related plasticity in the cortex.

L1 interneurons inhibit L2/3 PV$^+$ interneurons

How do foot-shock responses in L1 interneurons affect processing in the local microcircuit? There is evidence that L1 interneurons can inhibit interneurons in L2/3 during nicotinic activation[24]. Fast-spiking, PV$^+$ interneurons are the most abundant type of interneuron in the neocortex[3]. We injected a conditional adeno-associated virus (AAV) expressing a fluorescent marker (venus) into auditory cortex of PV-ires-Cre mice[33] to label these cells selectively (Fig. 3a). Targeted recordings revealed that PV$^+$ interneurons in L2/3 are tonically active under baseline conditions (5.9 ± 1.2 Hz, $n = 17$), similar to fast-spiking interneurons in awake, head-fixed mice[34]. Foot shocks caused prominent, long-lasting inhibition of firing in the majority of PV$^+$ interneurons (88%, Fig. 3b and Supplementary Fig. 8), while the remaining two neurons displayed an excitatory response (Supplementary Fig. 9). Inhibition of PV$^+$ interneurons was strongly reduced by the nAChR antagonists mecamylamine and methyllycaconitine (Fig. 3b and Supplementary Fig. 8), which also blocked excitation of L1 interneurons by foot shocks (Fig. 2c). Because PV$^+$ fast-spiking interneurons lack intrinsic responses to acetylcholine[10,35], this result is consistent with direct inhibition of PV$^+$ interneurons by L1 interneurons. In line with this interpretation, we observed morphological and functional synaptic contacts between L1 interneurons and PV$^+$ interneurons (Supplementary Fig. 10). In addition, the time course of foot-shock responses in the two populations matches (Supplementary Fig. 11). Taken together, these data indicate that L2/3 fast-spiking PV$^+$ interneurons are inhibited by L1 interneurons during foot shocks.

To test whether this mechanism is also engaged in awake, freely moving animals, we implanted mice with single-unit recording electrodes in the superficial layers of the auditory cortex (Fig. 3c and Supplementary Fig. 12). Putative interneurons were distinguished from putative pyramidal neurons using unsupervised cluster analysis (Fig. 3d and Supplementary Fig. 12). Recordings during fear conditioning confirmed that a large population of putative interneurons is inhibited during and after an aversive shock (Fig. 3e and Supplementary Fig. 12). The same neurons were activated by the CS, indicating that the shock removes feed-forward inhibition in pyramidal neurons during auditory input. A similar proportion of putative interneurons displayed either excitation or no response to shocks (Supplementary Fig. 12). These data are consistent with the interpretation that excitation of L1 interneurons by aversive stimuli serves to remove both spontaneous and feed-forward inhibition provided by PV$^+$ interneurons to surrounding pyramidal neurons in behaving mice.

Disinhibition of L2/3 pyramidal neurons

PV$^+$ basket cells provide strong, perisomatic inhibition to local pyramidal neurons[3,6,7,10]. To test directly whether disinhibition is the main effect of foot shocks in auditory cortex L2/3 pyramidal cells, we used whole-cell recordings. Foot shocks elicited a depolarization from rest in all neurons tested (5 ± 1.1 mV, $n = 6$, Fig. 4a). The amplitude increased at more depolarized membrane potentials (Supplementary Fig. 13), consistent with a response mediated by strong disinhibition and weak excitation[36]. Application of nAChR antagonists converted the foot-shock response to a net inhibition (Fig. 4a), suggesting an involvement of the disinhibitory circuit described here, and perhaps indicating that its block unmasks a component of inhibition recruited by foot shocks. Finally, recordings under conditions isolating inhibitory postsynaptic currents (IPSCs)[17] revealed a drastic reduction

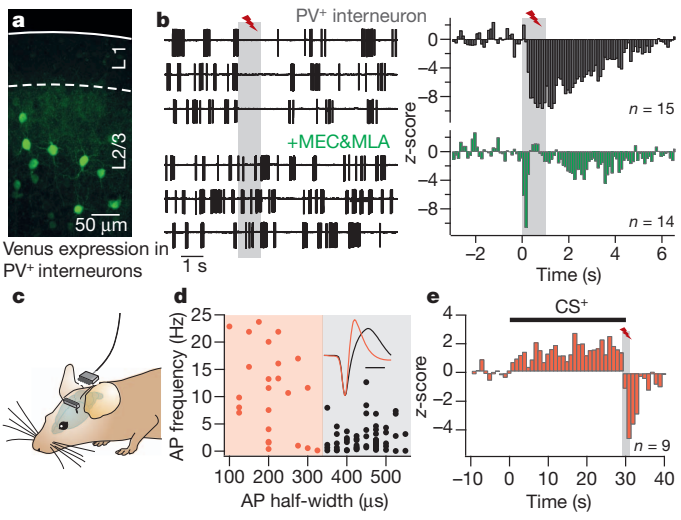

Figure 3 | Aversive shocks inhibit layer 2/3 PV$^+$ interneurons. **a**, Expression of venus in L2/3 PV$^+$ interneurons. **b**, Cell-attached recordings from PV$^+$ interneurons in control (top) show strong inhibition of spontaneous firing by foot shocks (left, example traces; right, population response). This response was strongly reduced in the presence of mecamylamine and methyllycaconitine (bottom). **c**, Single-unit recordings in the superficial layers of auditory cortex in freely behaving mice. **d**, Putative interneurons (red) were separated from putative pyramidal neurons (black) by unsupervised cluster analysis. Inset, example action potential (AP) waveforms (scale bar 400 µs). **e**, *z*-scored activity of putative interneurons showing inhibition by periorbital shocks during fear conditioning. Note recruitment by the CS$^+$ and subsequent inhibition by the shock ($n = 9$ of 24 putative interneurons, Supplementary Fig. 12).

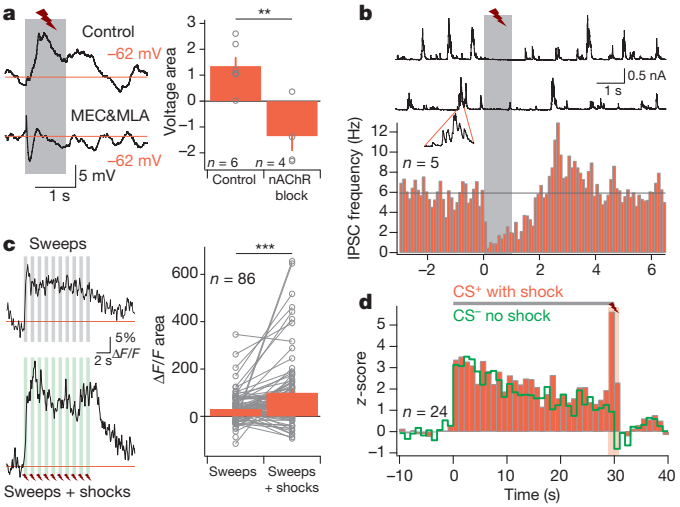

Figure 4 | Aversive shocks disinhibit L2/3 pyramidal neurons. **a**, Top left, *in vivo* whole-cell current-clamp recording of an auditory cortex pyramidal neuron during foot shocks. Bottom left, foot-shock response in the presence of mecamylamine and methyllycaconitine. Response area recorded at rest was reduced by nAChR antagonists (right). **b**, Whole-cell voltage-clamp recordings of inhibitory postsynaptic currents in pyramidal neurons show a strong reduction in IPSC frequency during and after foot shocks (top, example traces; bottom, population data, V_{hold} 0 to +20 mV). **c**, Left, example response of a L2/3 neuron to frequency-modulated sweeps (top) and sweeps paired with foot shocks (bottom) recorded with two-photon calcium imaging. Right, foot shocks caused a threefold enhancement of sweep response area in L2/3. **d**, Single-unit recordings of putative pyramidal neurons with significant response to the CS$^+$ in freely-behaving mice during fear conditioning. Note strong activation by coincidence of sweep and shock. Values are mean ± s.e.m. $^{**}P < 0.01$, $^{***}P < 0.001$. Statistical analysis in Supplementary Information.

of IPSC frequency during and after the foot shock (Fig. 4b). These results indicate that inhibition of PV^+ interneurons is a dominant influence shaping foot-shock responses in pyramidal neurons, and are in line with the observation that basal forebrain stimulation causes disinhibition of pyramidal cells[17].

Given that acetylcholine can affect many stages of neocortical information processing[8–11], we next aimed to determine how sensory input interacts with foot-shock-mediated disinhibition. We imaged calcium responses to tones in L2/3 of auditory cortex, and compared them to presentations of the same tones in conjunction with foot shocks (Fig. 4c and Supplementary Fig. 14). This experiment revealed that foot shocks cause a strong enhancement of the calcium signal integral, suggesting that tone/shock compounds elicit much greater activity than tones alone. A similar observation was made with extracellular recordings in freely moving mice, where coincidence of tone and shock excited putative pyramidal neurons much more than tone alone (Fig. 4d). This effect was highly supralinear in both experiments because shocks alone elicited almost no activity in these neurons (Supplementary Fig. 14). In summary, we provide evidence that L2/3 pyramidal neurons are disinhibited by aversive stimuli via inhibition of PV^+ interneurons.

Fear learning requires auditory cortex disinhibition

To determine whether activation of nAChRs contributes to fear learning, we applied mecamylamine and methyllycaconitine locally into the auditory cortex before fear conditioning (Fig. 5a and Supplementary Fig. 1). When tested 24 h later in drug-free state, this manipulation resulted in strongly reduced fear levels (Fig. 5b), consistent with a requirement for nicotinic activation of L1 interneurons. However, L1 interneurons are not the only circuit elements expressing nAChRs[8,9,11]. To test further whether disinhibition specifically during the foot shock contributes to fear learning, we used channelrhodopsin-2 (ChR-2)[37] expression in PV^+ interneurons (Fig. 5c and Supplementary Figs 15 and 16). Mice with chronic, bilateral optic fibre implantation (Fig. 5d) were subjected to differential fear conditioning in which optogenetic stimulation of PV^+ interneurons occurred during and for 5 s after the foot shock (Fig. 5e), the period during which we observed inhibition of these neurons (Fig. 3b). When tested 24 h later without optogenetic stimulation, these mice showed strongly reduced fear responses to the conditioned stimulus compared to sham-injected littermates (Fig. 5f). Reconditioning without optogenetic manipulation yielded normal fear learning (Fig. 5f). In addition, we ruled out the possibility that foot shock perception was perturbed by optogenetic stimulation and that laser illumination itself was perceived as a conditioned stimulus (Supplementary Fig. 17). Together, these data indicate that nicotinic disinhibition of the auditory cortex selectively during foot shock is required for associative fear learning.

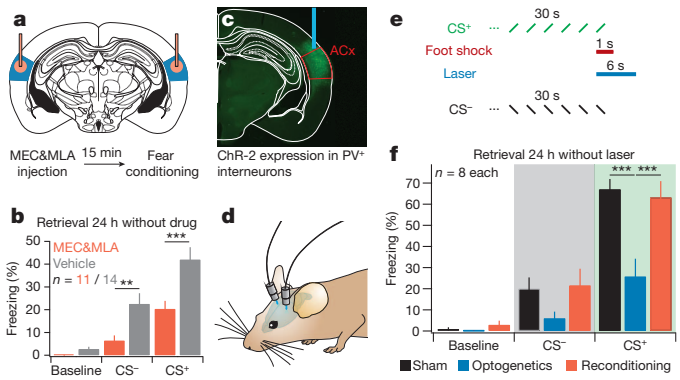

Figure 5 | Auditory cortex disinhibition is required for fear learning. **a**, Injection of mecamylamine and methyllycaconitine (red) into auditory cortex (blue) before fear conditioning. **b**, Drug-free freezing in a novel context one day after conditioning. Compared to vehicle-injected mice (grey), nAChR antagonism reduced freezing to both CS^- and CS^+ (red). **c**, Stimulation of ChR-2 expressing PV^+ interneurons (green) in auditory cortex (red) via an optic fibre (blue). **d**, Optogenetic manipulation in freely behaving mice. **e**, Differential fear conditioning protocol with optogenetic stimulation during and for 5 s after every foot shock. **f**, Freezing in a novel context without laser stimulation one day after conditioning. Compared to identically treated sham-injected littermates (black), virus-injected mice (blue) exhibit drastically reduced freezing to the CS^+. Reconditioning without optogenetic stimulation yielded strongly enhanced freezing (red) that was indistinguishable from sham. Values are mean ± s.e.m. $^{**}P < 0.01$, $^{***}P < 0.001$. Statistical analysis in Supplementary Information.

Discussion

Using targeted recordings from identified populations of auditory cortex neurons in conjunction with single-unit recordings, pharmacological and optogenetic manipulations in behaving mice, we have identified a disinhibitory microcircuit required for associative learning. Our data show that L1 interneurons play a central role in conveying information about an aversive stimulus to auditory cortex. Activity of L1 interneurons was tightly controlled by endogenous acetylcholine released from basal forebrain cholinergic projections, which determined baseline firing and acutely activated the majority of L1 interneurons during foot shocks, while a sub-set responded with inhibition. Given that all L1 interneurons express functional nAChRs[24] (Fig. 2), a likely source of this inhibition are synaptic interactions within L1 (ref. 25). Layer 1 contains several morphologically distinct subtypes of interneurons[22–25,38], and it remains to be determined whether foot-shock response type correlates with morphology. A strikingly similar activation by foot shocks was also observed in the primary visual cortex, which could underlie aspects of contextual fear learning and indicates that cholinergic activation of L1 interneurons may be a general feature of neocortical organization. Together, these results add to mounting evidence that L1 is a prominent locus of feedback signalling in the neocortex[27,28,32] and begin to define how feedback signals interact with thalamocortical feed-forward information during memory acquisition. Interestingly, L1 interneurons also receive prominent corticocortical feedback[27], and are responsive to dopamine[39] and serotonin[40], indicating that, depending on the nature of the learning task, different systems can feed into the microcircuit described here.

Foot shocks reduced both spontaneous and feed-forward perisomatic inhibition provided by basket cells, thus disinhibiting pyramidal neurons. Importantly, we cannot rule out that electrotonically remote dendritic sites received unchanged or even increased inhibition, for instance from L1 neurogliaform cells[25,38], which could serve to compartmentalize induction of synaptic plasticity. Nicotinic enhancement of inhibitory input to pyramidal neurons has been observed *in vitro*[11,41]. Therefore, the level of ongoing inhibition onto pyramidal neurons, as a prerequisite for disinhibition, may determine whether the net effect of nAChR activation is inhibitory or disinhibitory. Disinhibition is an attractive mechanism for learning because it is permissive for strong activation and concomitant plasticity induction, but not necessarily causative. Rather, the available sensory input at the time of the aversive stimulus can select the circuit elements for plasticity induction in a bottom-up fashion. In addition, other cholinergic actions like enhancement of thalamocortical transmission[11,42] and reduced GABA release from basket cell synapses[10] may have acted in synergy with the microcircuit described here to boost sensory responses.

Disinhibition of pyramidal neurons by foot shocks in turn probably gated the induction of activity-dependent plasticity in the auditory cortex[16,17] and at cortical afferents to the amygdala[18]. In parallel, cholinergic activation of L1 interneurons may also contribute to memory expression, because basal forebrain neurons acquire a conditioned response during learning[31,43]. Irrespective of the plasticity loci, our results delineate a role for the auditory cortex in fear conditioning to complex tones that goes beyond mere signalling of tone information to the amygdala[18–21]. Rather, we observe that stimulus convergence

and concomitant auditory cortex disinhibition are essential for fear learning. It is likely that the use of complex, naturalistic tones has emphasized the role of the auditory cortex[18], because fear conditioning to pure tones is often unaffected by auditory cortex lesions[19,21] (but see refs 19 and 20).

Beyond memory formation, cholinergic transmission is well known to mediate functions such as arousal and attention[30,31]. Interestingly, the transition from quiet wakefulness to active whisking is associated with a sharp drop in firing of fast-spiking interneurons in the barrel cortex[34], which is reminiscent of foot-shock responses in these neurons, and perhaps implies that cholinergic gating by inhibition of PV^+ interneurons is a general hallmark of active brain states.

METHODS SUMMARY

Male C57BL6/J mice (1.5 to 6 months old) were used. Full details of animals, materials and methods used for two-photon calcium imaging[44,45], patch-clamp[26] and single-unit recordings, pharmacological and optogenetic intervention[37] and behaviour[46] are provided in Methods.

Full Methods and any associated references are available in the online version of the paper at www.nature.com/nature.

Received 1 July; accepted 26 October 2011.
Published online 7 December 2011.

1. Martin, S. J. & Morris, R. G. New life in an old idea: the synaptic plasticity and memory hypothesis revisited. *Hippocampus* **12,** 609–636 (2002).
2. Hübener, M. & Bonhoeffer, T. Searching for engrams. *Neuron* **67,** 363–371 (2010).
3. Markram, H. *et al.* Interneurons of the neocortical inhibitory system. *Nature Rev. Neurosci.* **5,** 793–807 (2004).
4. Gabernet, L., Jadhav, S. P., Feldman, D. E., Carandini, M. & Scanziani, M. Somatosensory integration controlled by dynamic thalamocortical feed-forward inhibition. *Neuron* **48,** 315–327 (2005).
5. Wehr, M. & Zador, A. M. Balanced inhibition underlies tuning and sharpens spike timing in auditory cortex. *Nature* **426,** 442–446 (2003).
6. Freund, T. F. & Katona, I. Perisomatic inhibition. *Neuron* **56,** 33–42 (2007).
7. Kawaguchi, Y. & Kubota, Y. GABAergic cell subtypes and their synaptic connections in rat frontal cortex. *Cereb. Cortex* **7,** 476–486 (1997).
8. Lawrence, J. J. Cholinergic control of GABA release: emerging parallels between neocortex and hippocampus. *Trends Neurosci.* **31,** 317–327 (2008).
9. Bacci, A., Huguenard, J. R. & Prince, D. A. Modulation of neocortical interneurons: extrinsic influences and exercises in self-control. *Trends Neurosci.* **28,** 602–610 (2005).
10. Kruglikov, I. & Rudy, B. Perisomatic GABA release and thalamocortical integration onto neocortical excitatory cells are regulated by neuromodulators. *Neuron* **58,** 911–924 (2008).
11. Metherate, R. Nicotinic acetylcholine receptors in sensory cortex. *Learn. Mem.* **11,** 50–59 (2004).
12. Vogels, T. P. & Abbott, L. F. Gating multiple signals through detailed balance of excitation and inhibition in spiking networks. *Nature Neurosci.* **12,** 483–491 (2009).
13. Suga, N. & Ma, X. Multiparametric corticofugal modulation and plasticity in the auditory system. *Nature Rev. Neurosci.* **4,** 783–794 (2003).
14. Weinberger, N. M. Auditory associative memory and representational plasticity in the primary auditory cortex. *Hear. Res.* **229,** 54–68 (2007).
15. Quirk, G. J., Armony, J. L. & LeDoux, J. E. Fear conditioning enhances different temporal components of tone-evoked spike trains in auditory cortex and lateral amygdala. *Neuron* **19,** 613–624 (1997).
16. Ji, W., Suga, N. & Gao, E. Effects of agonists and antagonists of NMDA and ACh receptors on plasticity of bat auditory system elicited by fear conditioning. *J. Neurophysiol.* **94,** 1199–1211 (2005).
17. Froemke, R. C., Merzenich, M. M. & Schreiner, C. E. A synaptic memory trace for cortical receptive field plasticity. *Nature* **450,** 425–429 (2007).
18. LeDoux, J. E. Emotion circuits in the brain. *Annu. Rev. Neurosci.* **23,** 155–184 (2000).
19. Campeau, S. & Davis, M. Involvement of subcortical and cortical afferents to the lateral nucleus of the amygdala in fear conditioning measured with fear-potentiated startle in rats trained concurrently with auditory and visual conditioned stimuli. *J. Neurosci.* **15,** 2312–2327 (1995).
20. Boatman, J. A. & Kim, J. J. A thalamo-cortico-amygdala pathway mediates auditory fear conditioning in the intact brain. *Eur. J. Neurosci.* **24,** 894–900 (2006).
21. Romanski, L. M. & LeDoux, J. E. Bilateral destruction of neocortical and perirhinal projection targets of the acoustic thalamus does not disrupt auditory fear conditioning. *Neurosci. Lett.* **142,** 228–232 (1992).
22. Zhou, F. M. & Hablitz, J. J. Morphological properties of intracellularly labeled layer I neurons in rat neocortex. *J. Comp. Neurol.* **376,** 198–213 (1996).
23. Hestrin, S. & Armstrong, W. E. Morphology and physiology of cortical neurons in layer I. *J. Neurosci.* **16,** 5290–5300 (1996).
24. Christophe, E. *et al.* Two types of nicotinic receptors mediate an excitation of neocortical layer I interneurons. *J. Neurophysiol.* **88,** 1318–1327 (2002).
25. Chu, Z., Galarreta, M. & Hestrin, S. Synaptic interactions of late-spiking neocortical neurons in layer 1. *J. Neurosci.* **23,** 96–102 (2003).
26. Margrie, T. W. *et al.* Targeted whole-cell recordings in the mammalian brain *in vivo*. *Neuron* **39,** 911–918 (2003).
27. Gonchar, Y. & Burkhalter, A. Distinct GABAergic targets of feedforward and feedback connections between lower and higher areas of rat visual cortex. *J. Neurosci.* **23,** 10904–10912 (2003).
28. Cauller, L. J., Clancy, B. & Connors, B. W. Backward cortical projections to primary somatosensory cortex in rats extend long horizontal axons in layer I. *J. Comp. Neurol.* **390,** 297–310 (1998).
29. Rubio-Garrido, P., Perez-de-Manzo, F., Porrero, C., Galazo, M. J. & Clasca, F. Thalamic input to distal apical dendrites in neocortical layer 1 is massive and highly convergent. *Cereb. Cortex* **19,** 2380–2395 (2009).
30. Hasselmo, M. E. & Sarter, M. Modes and models of forebrain cholinergic neuromodulation of cognition. *Neuropsychopharmacology* **36,** 52–73 (2011).
31. Wenk, G. L. The nucleus basalis magnocellularis cholinergic system: one hundred years of progress. *Neurobiol. Learn. Mem.* **67,** 85–95 (1997).
32. Mechawar, N., Cozzari, C. & Descarries, L. Cholinergic innervation in adult rat cerebral cortex: a quantitative immunocytochemical description. *J. Comp. Neurol.* **428,** 305–318 (2000).
33. Hippenmeyer, S. *et al.* A developmental switch in the response of DRG neurons to ETS transcription factor signaling. *PLoS Biol.* **3,** e159 (2005).
34. Gentet, L. J., Avermann, M., Matyas, F., Staiger, J. F. & Petersen, C. C. Membrane potential dynamics of GABAergic neurons in the barrel cortex of behaving mice. *Neuron* **65,** 422–435 (2010).
35. Kawaguchi, Y. Selective cholinergic modulation of cortical GABAergic cell subtypes. *J. Neurophysiol.* **78,** 1743–1747 (1997).
36. Manookin, M. B., Beaudoin, D. L., Ernst, Z. R., Flagel, L. J. & Demb, J. B. Disinhibition combines with excitation to extend the operating range of the OFF visual pathway in daylight. *J. Neurosci.* **28,** 4136–4150 (2008).
37. Zhang, F., Aravanis, A. M., Adamantidis, A., de Lecea, L. & Deisseroth, K. Circuit-breakers: optical technologies for probing neural signals and systems. *Nature Rev. Neurosci.* **8,** 577–581 (2007).
38. Wozny, C. & Williams, S. R. Specificity of synaptic connectivity between layer 1 inhibitory interneurons and layer 2/3 pyramidal neurons in the rat neocortex. *Cereb. Cortex* **21,** 1818–1826 (2011).
39. Wu, J. & Hablitz, J. J. Cooperative activation of D1 and D2 dopamine receptors enhances a hyperpolarization-activated inward current in layer I interneurons. *J. Neurosci.* **25,** 6322–6328 (2005).
40. Foehring, R. C., van Brederode, J. F., Kinney, G. A. & Spain, W. J. Serotonergic modulation of supragranular neurons in rat sensorimotor cortex. *J. Neurosci.* **22,** 8238–8250 (2002).
41. Couey, J. J. *et al.* Distributed network actions by nicotine increase the threshold for spike-timing-dependent plasticity in prefrontal cortex. *Neuron* **54,** 73–87 (2007).
42. Gil, Z., Connors, B. W. & Amitai, Y. Differential regulation of neocortical synapses by neuromodulators and activity. *Neuron* **19,** 679–686 (1997).
43. Acquas, E., Wilson, C. & Fibiger, H. C. Conditioned and unconditioned stimuli increase frontal cortical and hippocampal acetylcholine release: effects of novelty, habituation, and fear. *J. Neurosci.* **16,** 3089–3096 (1996).
44. Stosiek, C., Garaschuk, O., Holthoff, K. & Konnerth, A. *In vivo* two-photon calcium imaging of neuronal networks. *Proc. Natl Acad. Sci. USA* **100,** 7319–7324 (2003).
45. Nimmerjahn, A., Kirchhoff, F., Kerr, J. N. & Helmchen, F. Sulforhodamine 101 as a specific marker of astroglia in the neocortex *in vivo*. *Nature Methods* **1,** 31–37 (2004).
46. Ciocchi, S. *et al.* Encoding of conditioned fear in central amygdala inhibitory circuits. *Nature* **468,** 277–282 (2010).

Supplementary Information is linked to the online version of the paper at www.nature.com/nature.

Acknowledgements We thank all members of the Lüthi laboratory for discussions and comments. We thank B. Kampa and T. Oertner for advice on two-photon imaging, R. Friedrich and J. Gründemann for comments on the manuscript, P. Argast, J. Lüdke and C. Müller for excellent technical assistance, H. Zielinska for preparation of artwork and S. Arber, Y. Yanagawa and K. Deisseroth for generously sharing materials. This work was supported by grants from the Swiss National Science Foundation (J.J.L. Ambizione; A.L.), the National Competence Center in Research (NCCR) of the Swiss Confederation on the synaptic basis of mental disorders, the French National Research Agency (C.H., ANR-2010-BLAN-1442-01), a Marie-Curie fellowship (J.J.L.), a Schering Foundation fellowship (S.B.E.W.), a Fonds AXA pour la Recherche fellowship (J.C.), the Aquitaine Regional Council (C.H.) and the Novartis Research Foundation.

Author Contributions J.J.L. initiated the project and performed most experiments and data analyses. S.B.E.W. established optogenetic manipulation. S.B.E.W. and P.T. helped with optogenetic experiments. E.M.M.M. performed and analysed *in vitro* experiments. P.T. performed and analysed *in vivo* pharmacology. J.C. and C.H. performed and analysed single-unit recordings. J.J.L. and A.L. conceived the project and wrote the manuscript. All authors contributed to the experimental design and interpretation, and commented on the manuscript.

Author Information Reprints and permissions information is available at www.nature.com/reprints. The authors declare no competing financial interests. Readers are welcome to comment on the online version of this article at www.nature.com/nature. Correspondence and requests for materials should be addressed to J.J.L. (johannes.letzkus@fmi.ch) or A.L. (andreas.luthi@fmi.ch).

METHODS

Animals. Male C57BL6/J mice (1.5–6 months old, Harlan and Janvier) were housed under a 12 h light/dark cycle, and provided with food and water ad libitum. Prior to fear conditioning, mice were individually housed for ≥ 7 days and habituated to handling ≥ 5 times. All animal procedures were executed in accordance with institutional guidelines and the prescribed authorities (Veterinary Department of the Canton of Basel-Stadt; Switzerland or Ministère de l'agriculture et de la forêt, 87-848, France and European Economic Community, EEC, 86-6091).

Head-fixed two-photon imaging and targeted patch-clamp recordings. Mice were sedated with chlorprothixene (5 mg kg^{-1}, intraperitoneal injection), kept warm on a hot-water bottle and after 10 min anaesthetized with urethane (0.9 g per kg, intraperitoneal injection). Core body temperature was maintained at 37.5 °C by a feedback-controlled heating pad (FHC). Mice were fixed in a stereotaxic frame (Kopf Instruments), and local analgesia was provided by injection of ropivacain under the scalp (10 mg ml^{-1}, Naropin, AstraZeneca). After retraction of the scalp, the location of the area of interest was determined as follows. Auditory cortex: 2.46 mm posterior of bregma, 4.5 to 4.7 mm lateral of midline; primary visual cortex: 3.16 mm posterior of bregma, 2.5 mm lateral of midline. A custom-built head-plate was glued to the skull with cyanoacrylate glue (Ultra Gel, Henkel) and dental cement (Paladur, Heraeus), and a small craniotomy was performed (2–3-mm diameter). The dura was retracted, the exposed cortical surface was superfused with normal rat ringer (NRR) containing (in mM): 135 NaCl, 5.4 KCl, 5 HEPES, 1.8 $CaCl_2$, pH 7.2 with NaOH), covered with agarose (1% type-III-A in NRR) and fixed with a coverslip. For two-photon calcium imaging, the membrane permeant dye Oregon Green BAPTA-1 acetoxymethyl ester (OGB-1, 1 mM in NRR with 8% DMSO and 2% pluronic F-127, Invitrogen) was pressure-ejected from a patch pipette under two-photon visualization. After 1 h, this lead to intracellular staining of virtually all cells in a diameter of approximately 300 μm[44]. Localization of the labelled area in auditory cortex was verified post hoc in slices. Sulforhodamine 101 (0.2 mM in NRR) was bath-applied for 5 min to the exposed cortex to counterstain glial cells[45]. Two-photon calcium imaging was performed using a scanning microscope (Fluoview 1000MPE, Olympus) coupled to a femtosecond-pulse infrared laser at 830 nm wavelength (MaiTai HP, Spectra-Physics). The beam was adjusted with a telescope to fill the back-focal plane of the ×20 water-immersion objective (0.95 numerical aperture, Olympus). Average power in the back-focal plane was <120 mW. Frames were acquired (Fluoview software, Olympus) at 15 Hz at depths below the pia ranging from 20 to 400 μm. Time stacks were processed offline using ImageJ to extract $\Delta F/F$ for each neuron. Foot shocks (1 s, direct current, 0.4 to 2 mA, 10–20 s interval) were delivered to the hindpaws. Frequency-modulated sweeps (logarithmically modulated between 5 and 15 kHz, 50 ms rise and fall) were generated (System3, Tucker Davis Technologies) and presented at 70 dB sound pressure level from an electrostatic speaker (ES1, TDT) mounted in front of the animal.

Two-photon-guided patch-clamp recordings were performed using patch pipettes of 4–10 MΩ resistance filled with NRR for cell-attached recordings, for whole-cell current-clamp recordings with intracellular solution containing (in mM): 130 K-methanesulphonate, 6.3 KCl, 20 Na_2-phosphocreatine, 4 Mg-ATP, 0.3 Na-GTP, 10 HEPES, 290 mOsm, pH 7.3 with KOH and for whole-cell voltage-clamp recordings with intracellular solution containing (in mM): 125 Cs-methanesulphonate, 2 CsCl, 10 Na_2-phosphocreatine, 4 Mg-ATP, 0.3 Na-GTP, 5 TEACl, 3.5 QX-314, 0.5 EGTA, 10 HEPES, 290 mOsm, pH 7.3 with CsOH. Pipette solutions were supplemented with Alexa 488 or Alexa 594 (25–50 μM, Invitrogen). Neurons of interest were identified by either marker expression (L1 interneurons in GAD67–GFP mice, PV^+ interneurons in PV-ires-Cre mice[33] injected with AAV conditionally expressing venus), or by imaging the 'shadows' created by neurons in dye-filled extracellular space in wild-type mice (L1 interneurons, L2/3 pyramidal neurons). L1 interneurons were located between 30 and 70 μm below the pia. Cell-attached and whole-cell recordings were established using a ×40 water-immersion objective (0.8 numerical aperture, Olympus) according to standard procedures[26]. Cell-attached recordings were performed in current-clamp or voltage-clamp configuration, and rejected when no action potential occurred during the entire length of the recording (≥5 min). Whole-cell current-clamp recordings were rejected when the series resistance exceeded 70 MΩ. Whole-cell voltage-clamp recordings were performed at 0–20 mV holding potential and rejected when the series resistance exceeded 50 MΩ. IPSCs were detected using a derivative threshold of 40 pA ms^{-1}. Pyramidal neurons were identified after dye filling by pyramidal morphology and spiny dendrites. Signals were recorded (Axopatch 200B, Molecular Devices or ELC-03XS, NPI), low-pass filtered at 20 kHz and digitized at 50 kHz (Digidata 1322A, Molecular Devices) using pClamp software (Molecular Devices). For cell-attached recordings, action potentials were detected based on amplitude. Peri-stimulus time histograms were computed across the entire population of recordings of a given type. Microstimulation of the basal forebrain (20 pulses of 0.2 ms duration delivered at 100 Hz) was performed using bipolar stimulating electrodes at the following coordinates: 0.8 mm posterior of bregma, 1.75 mm lateral of midline, 4.3 mm below cortical surface. Drugs were present in the bath solution throughout the experiment. Unless stated otherwise, chemicals were obtained from Sigma.

Surgery and local drug injection. Mice were anaesthetized with isoflurane (induction, 5%; maintenance, 1.5%) in oxygen-enriched air (Oxymat 3, Weinmann) and fixed in a stereotaxic frame (Kopf Instruments). Core body temperature was maintained at 36.5 °C by a feedback-controlled heating pad (FHC). Analgesia was provided by local injection of ropivacain under the scalp (Naropin, AstraZeneca) and systemic injection of meloxicam (100 μl of 5 mg ml^{-1}, intraperitoneal, Metacam, Boehringer-Ingelheim). Guide cannulae (26 gauge, with dummy screw caps, Plastics One) were implanted bilaterally to inject at the following coordinates: 2.46 mm posterior of bregma, ± 4.5 mm lateral of midline, 0.6 mm below cortical surface. Implants were fixed to the skull with cyanoacrylate glue (Ultra Gel, Henkel) and dental cement (Paladur, Heraeus). Mice were then given 1 week to recover from surgery, during which time they were handled ≥ 5 times to habituate them to the injection procedure. Fifteen minutes before fear conditioning, 32-gauge stainless steel injectors attached to 25 μl Hamilton syringes were inserted into the guide cannulae and an injection volume of 0.2 μl per hemisphere was delivered within 40 s using a microinfusion pump (Stoelting). Drug animals received bilateral injections of muscimol (100 ng per hemisphere) or a combination of mecamylamine (10 μg) and methyllycaconitine (10 μg) dissolved in NRR containing 1% fast green (Serva). Control mice were injected with vehicle solution only. In a subset of mice, fluorescent muscimol bodipy (625 μM in NRR with 5% DMSO) was injected after fear memory retrieval to quantify spread of the drug. After completion of the experiment, mice were transcardially perfused with 4% paraformaldehyde in phosphate-buffered saline (PFA), their brains extracted and post-fixed in paraformaldehyde overnight. For histological verification of the injection site, 60-μm coronal brain sections were made on a vibratome (Leica Microsystems) and imaged on a stereoscope (Leica Microsystems).

Virus injection and optogenetics. For labelling of PV^+ interneurons (Fig. 3a, b), an adeno-associated virus (AAV, serotype 2/7 (venus) or 2/9 (tdTomato), Vector Core, University of Pennsylvania) was used to deliver a DNA construct for conditional, Cre-dependent expression of venus or tdTomato. AAV (approximately 0.5 μl per hemisphere) was injected from glass pipettes (tip diameter 10–20 μm) connected to a picospritzer (Parker Hannifin Corporation) into the auditory cortex of PV-ires-Cre mice[33] at the following coordinates: 2.46 mm posterior of bregma, 4.5 mm lateral of midline, 0 to 1.1 mm below cortical surface. Experiments were performed after 0.5–3 months of expression time. For optical control of PV^+ interneurons (Fig. 5c–f), the same methodology was used for bilateral injection of a conditional AAV coexpressing channelrhodopsin-2 (ChR-2)[37] and venus (AAV2/7 EF1a::DIO-ChR2(H134R)-2A-NpHR-2A-Venus[47]) into the auditory cortex of PV-ires-Cre mice. These animals were additionally implanted with custom-built connectors holding optic fibres (0.48 numerical aperture, 200-μm diameter, Thorlabs). Fibre ends were inserted 200 μm into neocortex at the injection site. Implants were fixed to the skull with cyanoacrylate glue (Ultra Gel, Henkel) and dental cement (Paladur, Heraeus). After 2–4 months of expression time and habituation to handling, both implanted connectors were linked to a custom-built laser bench via optic fibres suspended over the conditioning context. This arrangement allowed the animals to move freely in the context. Stimulation of ChR-2 (<20 mW per implanted fibre) was delivered during and for 5 s after each foot shock (Fig. 5e) using a custom-built laser bench (laser: MBL473, 473-nm wavelength, CNI Lasers). One day after conditioning, mice were exposed to CS^+ and CS^- without optogenetic intervention in a neutral context. The optogenetic approach was previously validated *in vitro*[47] and *in vivo*[46], and here by acute extracellular recordings from auditory cortex of infected animals (Supplementary Fig. 16). Custom-built optrodes (optic fibre with 16-wire electrode attached) were lowered into the infected area. Laser pulses (300 ms) were delivered and recordings performed as detailed in section 'Extracellular recordings in freely behaving mice'. After completion of the experiment, mice were transcardially perfused with 4% paraformaldehyde. Brains were post-fixed in paraformaldehyde overnight at 4 °C, and cut into 80-μm thick coronal slices on a vibratome (Leica Microsystems). To improve the fluorescent signal, an immunostaining was performed. Slices were kept in blocking solution (3% BSA, 0.2% Triton in 0.1 M PBS) for 1 h at room temperature, before application of the primary antibody (Goat anti-GFP, Abcam; 1:500 in blocking solution) and incubated at 4 °C overnight. After washing, slices were incubated with secondary antibody (Alexa Fluor 488, donkey anti goat, Invitrogen; 1:1,000 in PBS with 3% BSA) at 4 °C overnight. After a final wash, slices were mounted on coverslips and imaged.

Behaviour. Fear conditioning and fear retrieval took place in two different contexts (context A and B). The conditioning and test boxes and the floor were cleaned before and after each session with 70% ethanol or 1% acetic acid, respectively. To score freezing behaviour, an automatic infrared beam detection system placed on the bottom of the experimental chambers (Coulbourn Instruments) was used. Mice were considered to be freezing if no movement was detected for 2 s and the measure was expressed as a percentage of time spent freezing. To ensure that our automatic system scores freezing rather than just immobility, we previously compared the values obtained with those measured using a classical time-sampling procedure during which an experimenter blind to the experimental conditions determined the mice to be freezing or not freezing every 2 s (defined as the complete absence of movement except for respiratory movements). The values obtained were 95% identical and the automatic detection system was therefore used throughout the experimental sessions. Conditioned stimuli for differential fear conditioning were 30-s trains of frequency-modulated sweeps (500 ms duration, logarithmically modulated between 5 and 15 kHz, 50 ms rise and fall) delivered at 1 Hz at a sound pressure level of 70 dB. The CS^+ (upsweep) was paired with a foot shock (1 s, 0.6 mA, 15 CS^+–foot-shock pairings; inter-trial interval: 20–180 s). The onset of the foot shock coincided with the onset of the last sweep in the CS^+. The CS^- (downsweep) was presented after each CS^+–foot-shock association, but was never reinforced (15 CS^- presentations, inter-trial interval: 20–180 s). On the next day, conditioned mice were submitted to fear retrieval in context B, during which they received 4 and 4 presentations of the CS^- and the CS^+, respectively.

Extracellular recordings in freely behaving mice. Surgical procedures are described earlier. Mice were secured in a stereotaxic frame and implanted with a pair of insulated silver wires (170-μm diameter) beneath the skin of each eyelid for delivery of periorbital shocks. In addition, mice were unilaterally implanted in the auditory cortex with a multi-wire electrode aimed at the following coordinates: 2.46 mm posterior of bregma, 4.5 mm lateral to midline, and 0.6 mm to 0.85 mm below the cortical surface. Electrodes consisted of 16 individually insulated, gold-plated nichrome wires (13 μm inner diameter, impedance 30 to 100 kΩ, Sandvik) contained in a 26-gauge stainless steel guide cannula. The wires were attached to a connector (18 pin, Omnetics). The implant was secured using cyanoacrylate adhesive gel. After surgery mice were allowed to recover for 7 days. Analgesia was applied before, and during the 3 days after surgery (Metacam, Boehringer-Ingelheim). Electrodes were connected to a headstage (Plexon) containing 16 unity-gain operational amplifiers. The headstage was connected to a 16-channel computer-controlled preamplifier (gain 100×, bandpass filter from 150 Hz to 9 kHz, Plexon). Neuronal activity was digitized at 40 kHz, bandpass filtered from 250 Hz to 8 kHz, and isolated by time–amplitude window discrimination and template matching using a multichannel acquisition processor system (Plexon). Single-unit spike sorting was performed using an off-line spike sorter (OFSS, Plexon). Principal component scores were calculated for unsorted waveforms and plotted on three-dimensional principal component spaces, and clusters containing similar valid waveforms were manually defined. A group of waveforms was considered to originate from a single neuron if it defined a discrete cluster in principal component space that was distinct from clusters for other units, and if it displayed a clear refractory period (1 ms) in auto-correlograms. Template waveforms were then calculated for well-separated clusters and stored for further analysis. To avoid analysis of the same neuron recorded on different channels, we computed cross-correlation histograms. If a target neuron displayed a peak of activity at a time that the reference neuron fired, only one of the two neurons was considered for further analysis. To separate putative inhibitory interneurons from putative excitatory pyramidal neurons we used an unsupervised cluster algorithm based on the Ward's method. Briefly, the Euclidian distance was calculated between all cell pairs based on the two-dimensional space defined by each cell's average spike width (measured from trough to peak) and baseline firing rate. An iterative agglomerative procedure was then used to combine cells into groups based on the matrix of distances such that the total number of groups was reduced to give the smallest possible increase in the within-group sum of square deviation. Mice were presented with the same conditioned stimuli used for fear conditioning (see above). The CS^+ was paired with a periorbital shock (2 s, 2.5 mA, 15 CS^+–shock pairings, inter-trial interval 20–180 s), which was used instead of foot shocks to minimize electrical artefacts in the recording. The onset of the periorbital shock coincided with the onset of the last sweep. The CS^- was presented after each CS^+ (15 CS^- presentations, inter-trial interval: 20–180 s). CS^+ and CS^- were counterbalanced across animals. At the conclusion of the experiment, recording sites were marked with electrolytic lesions before perfusion, and electrode locations were reconstructed with standard histological techniques

***In vitro* electrophysiology.** Coronal sections (300-μm thick) of auditory cortex were prepared from mice (6–8 weeks old) in ice-cold slicing artificial cerebrospinal fluid (ACSF) containing (in mM): 124 NaCl, 1.25 NaH_2PO_4, 10 $MgSO_4$, 2.7 KCl, 26 $NaHCO_3$, 2 $CaCl_2$, 10 Glucose, 4 ascorbate (95% O_2/5% CO_2). Slices were incubated for 45 min at 37 °C in an interface chamber, and then allowed to cool to room temperature. Recordings were performed at 34 °C under infrared videomicroscopy in ACSF containing (in mM): 124 NaCl, 1.25 NaH_2PO_4, 1.3 $MgSO_4$, 2.7 KCl, 26 $NaHCO_3$, 2 $CaCl_2$, 10 glucose, 4 ascorbate (95% O_2/5% CO_2). Whole-cell current-clamp recordings were performed with patch pipettes (4–10 MΩ resistance) filled with intracellular solution containing (in mM): 130 methanesulphonate, 6.3 KCl, 20 Na_2-phosphocreatine, 0.3 Na-GTP, 4 Mg-ATP, 10 HEPES, 5 biocytin, 290 mOsm, pH 7.3 with KOH. Signals were recorded (Multiclamp 700B, Molecular Devices), low-pass filtered at 10 kHz and digitized at 20 kHz (Digidata 1322A, Molecular Devices) using pClamp9 software (Molecular Devices). Signals were analysed using Igor Pro (Wavemetrics). The border between L1 and L2/3 was visually identified by the abrupt change in cell number, and only L1 interneurons at least 15 μm away from the border region were chosen for recordings. Local puff application of nicotine (100 μM, 20–80 ms duration) was delivered from a patch pipette connected to a picospritzer (Parker Hannifin Corporation). For paired recordings between L1 interneurons and L2/3 PV^+ interneurons, PV-ires-Cre mice were injected with an AAV (Vector Core, University of Pennsylvania) leading to Cre-dependent expression of tdTomato. Fluorescent PV^+ interneurons were identified using TillvisION (Till Photonics) and double recordings were performed as described above. Unless stated otherwise, drugs were bath-applied. To reveal morphology, slices were fixed in 4% paraformaldehyde (4 °C overnight), washed and stained for biocytin (4 days at 4 °C in PBS, 0.5–1% Triton-X, 0.2% Alexa (488, 568 or 680) streptavidin conjugate, Invitrogen). To identify putative synaptic contacts, this was combined with immunostaining against venus (see above) or tdTomato (Rabbit anti-RFP, MBL, Nunningen; 1:500 in blocking solution; Alexa Fluor 568, donkey anti-rabbit, Invitrogen; 1:1,000 in PBS with 3% BSA). Slices were mounted and confocal images acquired using an LSM700 confocal laser scanning microscope (Zeiss). Stacks were analysed using ImageJ (NIH) and single representative cells were reconstructed using Neurolucida software (MBF Bioscience). Putative synaptic contacts were scored when the axon of a L1 interneuron was located within 1 μm from a PV^+ dendrite or soma.

47. Tang, W. *et al.* Faithful expression of multiple proteins via 2A-peptide self-processing: a versatile and reliable method for manipulating brain circuits. *J. Neurosci.* **29,** 8621–8629 (2009).